

## Stabilization of Trapped-Particle Modes by Reversed-Gradient Profiles\*

W. M. Tang, P. H. Rutherford, H. P. Furth, and J. C. Adam

*Plasma Physics Laboratory, Princeton University, Princeton, New Jersey 08540*

(Received 16 June 1975)

Under certain modes of operation of very large tokamaks such as the proposed two-component torus (TCT), it is possible to create oppositely directed density and temperature gradients ( $\nabla n \cdot \nabla T < 0$ ) in the hotter central region of the plasma and the usual profile ( $\nabla n \cdot \nabla T > 0$ ) on the colder outer edge. Such configurations are found to be very favorable to stability against trapped-particle modes.

The two-component torus (TCT) concept<sup>1</sup> basically involves the injection of energetic neutral beams not only to heat the plasma but also to generate direct fusion reactions sufficient for net thermonuclear power production under conditions less restrictive than Lawson's criterion. A proposed mode of operation in such a system is injection followed by a mild compression of the plasma to the central position in the torus. The plasma density in the outer (blanket) region is then increased by introducing an influx of neutral gas immediately after compression. These neutrals are readily ionized before penetrating deep into the plasma and lead to the typical density and temperature profiles shown in Fig. 1. In this Letter, we note some advantages of this approach and focus in particular on the question of how the reversed radial density gradients produced here affect the trapped-particle instabilities.

Some of the principal benefits derived from operating with the "cold" transient plasma blanket are as follows: (1) There will be a reduction of the energy flux to the wall and limiter since the energy transported from the hot central plasma goes largely into heating the cold plasma

blanket. (2) In the blanket region, the energy of ions and charge-exchange neutrals may be reduced below the sputtering threshold (typically  $\sim 50$  eV). (3) Provided they obey the neoclassical-diffusion picture, the high- $Z$  impurities will accumulate toward the outside rather than in the hot central plasma, as long as the proton density peak lies in the blanket region. (4) The neutral density in the hot central plasma is actually reduced because the neutrals are readily ionized in the cool outer region. This is advantageous in that it reduces the losses due to charge exchange with high-energy beam ions.

In light of the preceding beneficial effects, it becomes important to address the question of how the mode of operation described will affect the microinstability picture. Numerical results obtained from a tokamak radial-transport code<sup>2</sup> indicate that the reversed-density-gradient region typically falls within the banana regime (where the effective collision frequency  $\nu_{\text{eff}}$  is less than the trapped-particle bounce frequency  $\omega_b$ ). In what follows, we will analyze the effect of this inverted profile on the trapped-electron and trapped-ion instabilities.

The trapped-electron modes<sup>3</sup> are drift-type instabilities with characteristic frequencies falling between the thermal ion and electron bounce frequencies ( $\omega_{bt} < \omega < \omega_{be}$ ). These modes, which do not require the ions to be in the banana regime, are driven unstable by dissipation from electron collisions in the presence of temperature gradients. For the usual case,  $\nabla n \cdot \nabla T > 0$ , it was believed that the instabilities could be stabilized in tokamaks by attainable levels of magnetic shear strength.<sup>4,5</sup> However, in a recent calculation<sup>6</sup> it was pointed out that Landau resonances associated with the  $\nabla B$  drift of the trapped electrons can lead to much larger growth rates and thus render stabilization far more difficult. In the analysis which follows, this will be taken into account together with previously considered effects such

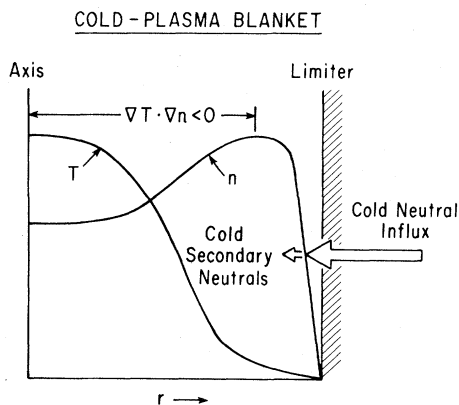


FIG. 1. Schematic density and temperature profiles with outward plasma-density peak created by neutral-gas influx.

as shear<sup>5</sup> and infinite ion gyroradius.<sup>7</sup>

To obtain the dispersion relation, we follow the usual approach of solving the Vlasov-Maxwell equations in the electrostatic limit with a Krook model for collisions.<sup>5</sup> After obtaining approximate forms of the perturbed distribution function for ions and electrons (in limit  $\omega/\omega_{be}$ ,  $\omega_{bi}/\omega$  small), the quasineutrality condition,  $\sum_j e_j \int d^3v f_j = 0$ , is invoked to yield the basic mode equation. In the radially local limit, the most unstable situation occurs at the rational surfaces where the stabilizing ion Landau-damping effects are negligible. The mode structure (to lowest order) is determined by an integral equation which can be solved by a variational procedure maximizing the growth rate.<sup>8</sup> The assumption that  $\bar{\varphi} \approx \varphi$  ( $\bar{\varphi}$  is the potential averaged over trapped-particle orbit) simplifies the analysis and still gives the growth rate to within about a factor 2 of the variational result. The resultant dispersion relation then takes the form

$$Q(\omega, b) \equiv 1 + \tau - \left( \tau + \frac{\omega_*}{\omega} \right) \Gamma_0 - \eta_i \frac{\omega_*}{\omega} b (\Gamma_1 - \Gamma_0) - (2\epsilon)^{1/2} \left\langle \frac{\omega - \omega_* \left[ 1 + \eta_e (E/T_e - \frac{3}{2}) \right]}{\omega - \omega_{De} (E/T_e) + i\nu_{eff,e} (E/T_e)^{-3/2}} \right\rangle = 0, \quad (1)$$

where  $\omega_* = ck_{\perp} T_e / eBr_n$ , with  $r_n = (d \ln n / dr)^{-1}$ ;  $\tau = T_e / T_i$ ;  $\Gamma_n = I_n(b) \exp(-b)$ , with  $I_n$  a modified Bessel function;  $b = k_{\perp}^2 \rho_i^2 / 2$ ;  $\rho_i = v_i / \Omega_i$ ;  $v_i = (2T_i / M_i)^{1/2}$ ;  $\eta_j = d \ln T_j / d \ln r_j$ ;  $\epsilon = r/R$  (local inverse aspect ratio);  $\nu_{eff,e} = \nu_e / \epsilon$ ;

$$\langle A \rangle \equiv (2/\pi)^{1/2} T_e^{3/2} \int_0^{\infty} dE E^{1/2} \exp(-E/T_e) A;$$

and  $\omega_{De} \approx \omega_* r_n / R$ .<sup>9</sup>

Because the  $\omega_{De}$  resonances are important, the usual perturbative approach<sup>5</sup> to solving Eq. (1) is not applicable for the smaller values of the collision frequency. We therefore solved this dispersion relation numerically and have displayed the results in Fig. 2. Here we plot the maximum growth rates (normalized by the average trapped-electron bounce frequency,  $\omega_{be}^T$ ) against the banana-regime parameter,  $\nu_* \equiv \nu_{eff,e} / \omega_{be}^T$ . For each value of  $\nu_*$ , growth rates were calculated over a wide range in  $k_{\perp}$  and the largest answers plotted in Fig. 2. In these calculations, we have taken  $r_n/R \approx \epsilon = \frac{1}{4}$ ,  $\tau = 1$ , and  $\eta_e = \eta_i = \pm 1$ . Positive values of  $\eta_{e,i}$  correspond to the normal profile

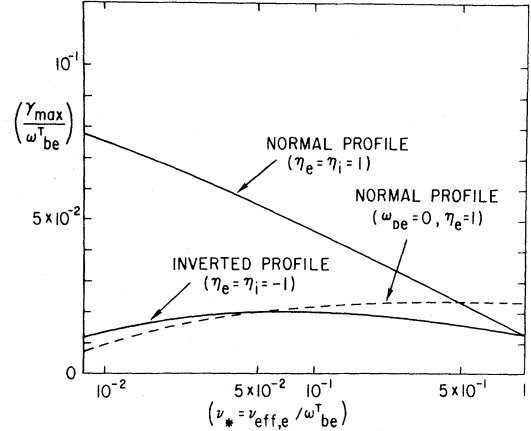


FIG. 2. Maximum trapped-electron-mode growth rates for normal ( $\eta_{i,e} > 0$ ) and inverted ( $\eta_{i,e} < 0$ ) profiles with  $r_n/R \approx \epsilon = \frac{1}{4}$  and  $T_e = T_i$ . Dashed lines indicate results ignoring  $\omega_{De}$  terms with  $\eta_i = 0$ .

which leads to the strong enhancement of the growth rate shown on the graph. On the other hand, the inverted-profile situation ( $\eta_{e,i}$  negative) leads to maximum growth rates which are much reduced and are comparable to the answers obtained ignoring the drift resonances ( $\omega_{De} = 0$ ). These important destabilizing resonances are rendered ineffective for the inverted density gradient situation because the diamagnetic drifts,  $\omega_*$  (and therefore the mode frequency,  $\omega$ ), are reversed, while the curvature drifts,  $\omega_{De}$ , remain unaffected. Hence, the destabilizing resonances can now occur only between the waves and the very small population of trapped electrons with average good-curvature drifts ( $\omega_{De} < 0$ ).

Turning now to the question of shear stabilization of these modes we consider the radial eigenmode equation<sup>5</sup> and include the curvature-drift terms. Solving this Weber-type differential equation invoking the usual outgoing-wave boundary conditions leads to the following eigenvalue equation:

$$Q(\omega, b) = -i(2\hat{n} + 1) \left( \frac{L_n}{L_s} \right) \left( \frac{\omega_*}{\omega} \right) (\Gamma_0 - \Gamma_1)^{1/2} \left\{ 1 + \frac{\omega_*}{\omega\tau} \left[ 1 + \eta_i \left( \frac{\Gamma_0}{\Gamma_0 - \Gamma_1} - 2b \right) \right] \right\}^{1/2} \times \left( 1 + \frac{\omega_*}{\omega\tau} \left\{ 1 + \eta_i \left[ 1 - b \left( 1 - \frac{\Gamma_1}{\Gamma_0} \right) \right] \right\} \right)^{1/2}, \quad (2)$$

where  $\hat{n}$  is the radial eigenmode number,  $b = k_{\theta}^2 \rho_i^2$ ,  $k_{\theta} = lq/r$ ,  $q$  is the safety factor,  $l$  is the toroidal

mode number,  $L_n \equiv |d \ln n / dr|^{-1}$ , and the shear length  $L_s \equiv |(\epsilon/q)(d \ln q / dr)|^{-1}$ . The result here requires the  $\eta_i$ -dependent terms (under the square-root operations) to remain positive. This condition is always met for normal profiles ( $\eta_i > 0$ ), and is also satisfied for inverted profiles ( $\eta_i < 0$ ) provided  $-\eta_i \lesssim 2$  (which is the situation considered in this Letter). The eigenvalues are again evaluated numerically and the critical magnetic shear required for stability is plotted against  $\nu_*$  in Fig. 3 [ $L_s/L_n < (L_s/L_n)_{\text{crit}}$  for stability]. Here it is shown that for normal profiles the shear criterion is difficult to satisfy, but that for the reversed-gradient situation the required shear strengths fall in an attainable range ( $L_s/L_n \sim 10$ ).

The trapped-ion modes<sup>3</sup> are unstable drift-type waves which require both the electrons and the ions to be in the banana regime. Since the radially local treatment of these modes gives the most stringent stability criteria, we follow this type of analysis in determining the influence of the inverted profiles. As shown in earlier work,<sup>10</sup> the destabilizing electron-collisional-growth term takes the form

$$\gamma_e = c_1 (\omega_*^2 / \nu_e) (1 - |\omega_0 / \omega_*| + 1.4 \eta_e), \quad (3)$$

where  $c_1$  is a factor independent of  $\omega_*$ , and  $\omega_0$  is the lowest-order mode frequency with  $|\omega_0 / \omega_*| \simeq \frac{1}{4}$  typically. Thus, for inverted profiles ( $\eta_e < 0$ ) the usually destabilizing temperature-gradient term now makes the electron collisions stabilizing for  $-\eta_e > \frac{1}{2}$ .

To ensure complete stabilization under such conditions, it is still necessary to examine the influence of the reversed density gradients on the previously considered linear damping mechanisms.<sup>10</sup> As shown below, these stabilizing effects are all enhanced: (1) Ion collisional damping is given by

$$\gamma_i = -c_2 \left| \frac{\nu_i}{\omega_0} \right| \left[ \ln \left( \alpha \left| \frac{\omega_0}{\nu_i} \right|^{1/2} \right) \right]^{-3/2} \left( 1 + \left| \frac{\omega_0}{\omega_*} \right| - 0.6 \eta_i \right), \quad (4)$$

where  $c_2$  and  $\alpha$  are factors independent of  $\omega_*$ . For inverted profiles ( $\eta_i < 0$ ), the  $\nabla T_i$  contribution is stabilizing and hence can never make  $\gamma_i$  destabilizing. (2) Bounce resonance damping due to circulating and trapped ions is given approximately by

$$\gamma_{LD} = -c_3 |\omega_0^4 / (\omega_{Di}^T)^3| [1 + |\omega_0 / \omega_*| (1 - \frac{3}{2} \eta_i)], \quad (5)$$

with  $c_3$  a factor independent of the sign of  $\omega_*$ . Again the  $\nabla T_i$  contribution is stabilizing for reversed density gradients and thus ensures that  $\gamma_{LD}$  is always stabilizing. (3) Ion-drift resonance damping for inverted profiles can be approximated by

$$\gamma_{\text{drift}} = -c_4 \int_{\xi_0}^1 d\xi [1 + |\omega_* / \omega_0| (1 - \frac{3}{2} \eta_i) + \eta_i / g(\xi)] G(\xi), \quad (6)$$

where  $\xi$  is a velocity-space pitch-angle variable,  $g(\xi)$  and  $G(\xi)$  are positive functions of  $\xi$ ,  $c_4$  is a factor independent of the sign of  $\omega_*$ , and  $\xi_0 < 0.2$  typically. This again is always a stabilizing effect with  $\eta_i < 0$  and is much enhanced over the normal-profile situation. The reason is similar to that given earlier for trapped-electron-drift resonant effects; i.e., the reversed density gradients change the sign of  $\omega$  without affecting  $\omega_{Di}$ , so that the resonances now occur with the much larger population of trapped ions with average bad  $\nabla B$  drifts ( $\omega_{Di} > 0$ ).

In summary, we have noted in this Letter that there are many advantages associated with using the cold-plasma-blanket approach in operating future large tokamaks, and that the reversed density gradients generated by this technique exert a strong stabilizing influence on the trapped-particle modes. In the case of trapped-electron modes the inverted profiles do not eliminate the instabilities, but do have the effect of significantly re-

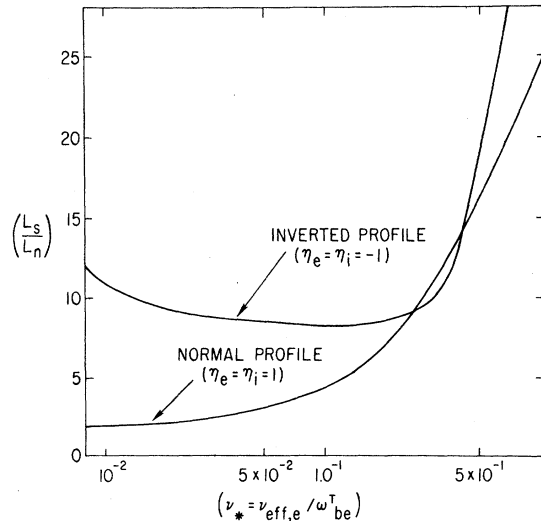


FIG. 3. Critical magnetic shear lengths required to stabilize trapped-electron modes for normal ( $\eta_{i,e} > 0$ ) and inverted ( $\eta_{i,e} < 0$ ) profiles with  $r_n/R \simeq \epsilon = \frac{1}{4}$  and  $T_e = T_i$ .

ducing the growth rates by rendering ineffective the destabilizing electron  $\nabla B$ -drift resonances. Under such conditions shear stabilization of the modes appears achievable, provided the temperature gradients are not too severe. For trapped-ion instabilities, our calculations indicate that the reversed gradients should easily stabilize the modes. Here we find a strong reduction of the growth term, together with a pronounced enhancement of all damping effects. It should be pointed out, however, that ordinary dissipative and collisionless drift instabilities<sup>3</sup> (outside the banana regime) are further destabilized by inverted gradients. In particular, untrapped-electron resonances, which drive the unstable collisionless drift waves and also affect the trapped-electron modes,<sup>11</sup> can be exacerbated by such profiles. Such effects together with estimates of transport associated with the mode of operation described in the Letter are currently under investigation. As a final point, it is of interest to note that in recent studies of trapped-electron-related phenomena in the Princeton FM-1 spherator experiment, a marked reduction of unstable fluctuations was observed when oppositely directed density and temperature gradients were created.<sup>12</sup>

\*Work supported by the U. S. Energy Research and Development Administration under Contract No. E (11-1)-3073.

<sup>1</sup>J. M. Dawson, H. P. Furth, and F. H. Tenney,

Phys. Rev. Lett. **26**, 1156 (1971); H. P. Furth and D. L. Jassby, Phys. Rev. Lett. **32**, 1176 (1974).

<sup>2</sup>P. H. Rutherford *et al.*, to be published.

<sup>3</sup>B. B. Kadomtsev and O. P. Pogutse, *Reviews of Plasma Physics*, edited by M. Leontovich (Consultants Bureau, New York, 1970), Vol. 5.

<sup>4</sup>A. A. Galeev, in *Proceedings of the Third International Symposium on Toroidal Plasma Confinement, Garching, Germany, 26-30 March 1973*, (Max-Planck-Institut für Plasmaphysik, Garching, Germany, 1973), paper E1-I.

<sup>5</sup>W. Horton, Jr., *et al.*, in *Proceedings of the Fifth International Conference on Plasma Physics and Controlled Nuclear Fusion Research, Tokyo, Japan, 1974* (International Atomic Energy Agency, Vienna, Austria, 1975), paper CN-33/A14-3.

<sup>6</sup>J. C. Adam, W. M. Tang, and P. H. Rutherford, Princeton Plasma Physics Laboratory Report No. MATT 1156, 1975 (to be published).

<sup>7</sup>C. S. Liu, M. N. Rosenbluth, and W. M. Tang, Princeton Plasma Physics Laboratory Report No. MATT 1125, 1975 (to be published).

<sup>8</sup>W. M. Tang, P. H. Rutherford, and E. A. Frieman, to be published.

<sup>9</sup>The orbit-averaged curvature-drift frequency appearing here has a weak dependence on the velocity-space pitch angle ( $\lambda = \mu/E$ ) which is ignored. This weak dependence is illustrated in Ref. 3, page 265.

<sup>10</sup>W. M. Tang, Phys. Fluids **17**, 1249 (1974).

<sup>11</sup>For normal profiles, the stabilizing effect of untrapped-electron resonances on the trapped-electron modes is calculated in W. M. Tang *et al.*, Princeton Plasma Physics Laboratory Report No. MATT 1153, 1975 (to be published).

<sup>12</sup>S. Ejima and M. Okabayashi, Phys. Fluids **18**, 904 (1975).

## Magnetic Fields Due to Resonance Absorption of Laser Light\*

J. J. Thomson, Claire Ellen Max, and Kent Estabrook

Lawrence Livermore Laboratory, University of California, Livermore, California 94550

(Received 2 April 1975)

We discuss the generation of dc magnetic fields due to the resonant excitation of plasma waves by an obliquely incident, plane-polarized laser beam. We show that the averaged forces on the electrons due to the plasma waves produce magnetic fields perpendicular to the plane of incidence. Megagauss field levels may be reached. Computer simulations verify our theoretical predictions.

Recently evidence has grown that megagauss magnetic fields can be generated as a result of the interaction of intense laser light with plasma.<sup>1,2</sup> Fields of this magnitude can have a substantial effect on the transport properties of laser-fusion plasmas.<sup>3</sup> Thus, it is important to understand their sources and characteristics.

Most theoretical work on this subject has con-

centrated on the fields due to the thermoelectric current.<sup>1,4</sup> In the present work, we investigate field generation that is an intrinsic part of resonance absorption. The latter process occurs when plane-polarized light is obliquely incident on a plasma with a density gradient. Since a focused laser spot contains rays with a variety of angles, resonance absorption is a ubiquitous phe-